Interfacial Characterization and Optimal Preparation of Novel Bamboo Plastic Composite Engineering Materials

Wei Song,[a,b,c] Fang Zhao,[a] Xuefei Yu,[a] Cuicui Wang,[a] Wenbang Wei,[a,b,c] and Shuangbao Zhang [a,b,c,*]

To blaze new trails for utilizing forestry processing residue, higher plant content biocomposites were proposed based on a combination of moso bamboo flour/silane KH550/high density polyethylene (HDPE), and the materials were characterized by diffractometry, spectroscopy, microscopy, and calorimetry. During surface modification, reactions between bamboo and silane occurred on the lignin aldehyde group. After 6 wt% KH550 treatment, crystallinity of bamboo was increased by 1.11 %, and melting temperature and enthalpy of the composite rose by 2.37 °C and 5.27 J/g, agreeing with improved interface morphology. Increasing in thickness from 3 to 9 mm, the physical and mechanical properties of composite were improved overall. Bamboo content caused the biggest influence, while thickness swelling exhibited the greatest susceptibility. Increasing the bamboo ratio boosted flexural and tensile properties, but it compromised toughness and water resistance, while silane and moulding parameters featured complicated relationships regarding performances. Combining an artificial neural network (ANN), KH550 3 wt%, moulding temperature of 180 °C, and a time of 8 min endowed 9 mm composites of 70 wt% bamboo with performance comparable to load bearing MDF in GB/T 11718. This research helped establish the first "Bamboo Plastic Composite" standard proposed by the authors for the Chinese forestry industry.

Keywords: Bamboo plastic composite; Silane coupling agent; Compatibilization; Interface; Artificial neural network

*Contact information: a: MOE Key Laboratory of Wooden Material Science and Application, College of Materials Science and Technology, Beijing Forestry University, Beijing 100083, China; b: Beijing Key Laboratory of Wood Science and Engineering, College of Materials Science and Technology, Beijing Forestry University, Beijing 100083, China; c: MOE Engineering Research Center of Forestry Biomass Materials and Bioenergy, College of Materials Science and Technology, Beijing Forestry University, Beijing 100083, China; *Corresponding author: shuangbaozhangj5@163.com*

INTRODUCTION

Fiber-reinforced polymer composites are gaining widespread popularity in automobile, aircraft, and building material domains, where fillers often include synthetic and natural fibers (Cheng *et al.* 2015). For the former, aramid, carbon, glass, and graphite fibers serve as excellent reinforcements, but the scarcity of petroleum resources, relatively complicated processes, high energy consumption, high initial cost, and poor biodegradability have caused their recession (Lu *et al.* 2014; Zakikhani *et al.* 2014). For the latter, the renewable, inexpensive, biocompatible characteristics, and desirable performance have allowed natural fibers to gain more impetus (Saba *et al.* 2015). Despite a lower density, a content of over 60 wt% cellulose (Young's modulus 140 to 250 GPa) endows natural fiber with 6 to 80 GPa modulus, which is comparable to glass fibers (Yeh

et al. 2015). The effectiveness of some lignocellulosic fibers (*e.g.*, wood, bamboo, jute) in load-bearing material has been partly demonstrated (Hebel *et al.* 2014; Liu *et al.* 2014a; Peng *et al.* 2014, 2015). However, both thermoset (*e.g.*, formaldehyde resin) and thermoplastic (*e.g.*, polyolefin) polymeric materials can serve as the matrix (Cheng *et al.* 2015), while over 80% of global consumption would be thermoplastics (Faruk *et al.* 2012). Due to growing environmental consciousness, thermoplastics are expected to become more environmentally friendly adhesives and to receive widespread application in the future (Fang *et al.* 2014). Overall, natural fibers reinforced with thermoplastic material would present a lower carbon footprint, and become a more sustainable alternative (Yeh *et al.* 2015).

However, the inherent incompatibility of polar, hydrophilic natural fibers with a nonpolar, hydrophobic polymer matrix causes a poor interfacial adhesion in their composite (Lu *et al.* 2014; Lei *et al.* 2015; Yeh *et al.* 2015). Once stress fails to be properly transferred between two phases, physical and mechanical properties can be compromised (Li *et al.* 2013), thus restricting its construction and building applications (Hung *et al.* 2012). Currently, fiber surface modification has been widely used in interfacial compatibilization. Corona or plasma discharge, inorganic or organic filling (*e.g.*, calcium carbonate, organo-montmorillonite), and heat treatment (Du *et al.* 2014; Liu *et al.* 2014b; Cheng *et al.* 2015; Yeh *et al.* 2015) are typical physical approaches. For instance, the tensile strength of bamboo fiber/polypropylene (PP) composite is enhanced by 10.4% after 0.2 mol/L of $CaCO_3$ *in situ* deposition (Cheng *et al.* 2015). Acetylation, benzoylation, enzyme, alkali, and various other compatibilizer treatments are commonly used chemical methods (Hung *et al.* 2012; Mamun and Bledzki 2013; Luo *et al.* 2014; Wang *et al.* 2014; Yeh *et al.* 2015). The tensile strength of bamboo flour/polylactic acid (PLA) composite is heightened by 44% with 15 hpr PLA grafting glycidyl methacrylate (GMA) addition (Wang *et al.* 2014). Featuring a bi-functional structure, silane coupling agent would build chemical bridges between polymer and biofiber, which has the potential for effective compatibilization (Li *et al.* 2014). To date, several silanes (*e.g.*, A-171, KH550, and KH560) have been successfully applied in a wide range of combinations, such as rice husk/PP (Yeh *et al.* 2015), bamboo cellulose/poly (L-lactic acid) (PLLA) (Lu *et al.* 2014), corn fiber/PLA (Luo *et al.* 2014). Shear strength and water absorption of poplar/high density polyethylene (HDPE) plywood was improved by 293% (↑) and 34% (↓), respectively, through 2 wt% A-171 spraying (Fang *et al.* 2014).

Among the various combinations, moso bamboo flour/HDPE composites have potential to achieve greater prominence in developing countries such as China. Nowadays, moso bamboo is very popular for structural use, and 85% of moso bamboo grows in China, covering 70% of Chinese bamboo forests (Li *et al.* 2012). Generally, bamboo features many advantages. The first is wide abundance. At least 75 genera and 1250 species have been discovered, while 24 million ha of bamboo forest exists in 16 Asian countries (Correia *et al.* 2014). China, as a "bamboo kingdom," retains the longest cultivating history, largest forest acreage, greatest abundance of species, and highest production in the world (Zhao 2012). Another advantage is that as the fastest-growing and highest-yielding redeemable material, bamboo achieves a maximum height (15 to 30 m) in 2 to 4 months, maturity in 6 to 8 months (<5 % of most woods), and optimal mechanical properties in 3 to 4 years; it also produces biomass 4 times faster than timber (Huda *et al.* 2012; Li *et al.* 2012; Verma *et al.* 2014). The third advantage is bamboo's excellent performance. Known as "natural glass fiber," bamboo possesses the lowest density (0.9 g/cm^3<1.45 g/cm^3 of jute and 2.5 g/cm^3 of glass), highest strength, a larger

aspect ratio (than pine), a higher strength to weight ratio (than concrete, timber, and steel), and good wear resistance among the natural fibers (Huda *et al.* 2012; Li *et al.* 2012; Zhou *et al.* 2012). Furthermore, bamboo contains 60 wt% cellulose, with a smaller microfibrillar angle of 2 to 10°, thereby facilitating matrix reinforcement (Abdul Khalil *et al.* 2012). Finally, bamboo fiber is about 10 times cheaper than glass fiber (Huda *et al.* 2012). Unfortunately, under the current processing capacity of China, over 60 wt% of bamboo would become residue such as flour (whose units suffer greater damage and are different from general fiber), thus posing a threat to the environment (Zhou *et al.* 2012). Similarly, HDPE is a major product of the Chinese chemical industry and serves as a commonly-used matrix of polymer composite and key source of white pollution (Du *et al.* 2014; Fang *et al.* 2014; Li *et al.* 2014; Ren *et al.* 2014). Therefore, the high value-added utilization of a moso bamboo flour/HDPE system holds promise to provide huge economic, social, and ecological benefits.

However, to the authors' best knowledge, the application of silane to this combination has been barely reported on, with the loading level of natural fiber among previous works generally lower (<50%), thereby failing to make full use of potential resources (Fang *et al.* 2014; Lu *et al.* 2014; Luo *et al.* 2014; Yeh *et al.* 2015). Since data findings and study conclusions (especially the mechanism regarding interfacial bonding) may change greatly under different materials and processes, targeted research on this silane modified bamboo plastic composite is undoubtedly very necessary (Zakikhani *et al.* 2014).

Some explorations have recently been conducted by the authors' team to deepen the understanding of biocomposites in the course of investigating various bamboo-based engineering materials (Zhao 2012; Cheng *et al.* 2014; Wei *et al.* 2014; Cheng *et al.* 2015). Considering that, the objectives of this paper are to:

1) propose a technological route that applies to fabricating higher plant content biocomposites based on the combination of moso bamboo flour/silane KH550/HDPE;
2) reveal the compatibilization effects of KH550 on bamboo plastic interface in terms of crystalline structure, microscopic morphology, and thermal stability;
3) investigate the relationship between the manufacturing process and physical/ properties through orthogonal experiments; and
4) optimize the composite performance to demonstrate its potential in construction applications by virtue of artificial intelligence (AI).

EXPERIMENTAL

Raw Materials

Moso bamboo flour (*Phyllostachys edulis*; over 6 years old, 60 mesh, and made from forestry processing residue) was purchased from Deqing Linpai Co., Ltd, China. HDPE, with the following characteristics: 5000S, density 0.95 g/cm^3, melting point 131 °C, melt flow rate 0.82 g/10 min at 190 °C/2.16 kg, made from recycled plastic after screening, cleaning, and extruding, was supplied by Dongguan Changyuan Co., Ltd, China. Silane coupling agent, γ-aminopropyltriethoxysilane (commercial code: KH550, purity ≥97.0 %, and density 0.944 to 0.950 g/cm^3 at 20 °C) was provided by Nanjing Union Silicon Co., Ltd, China.

Experimental Design

First, an adequate range of technological parameters during composite preparation was determined. Then, the compatibilization effects of KH550 on the bamboo plastic interface were confirmed by applying X-ray diffractometry (XRD), Fourier transform infrared spectroscopy (FT-IR), scanning electron microscopy (SEM), and differential scanning calorimetry (DSC). Next, the impacts of raw material and moulding processes on the composite were further investigated. Since orthogonal experiments feature uniform dispersion and neat comparability, a L_9 (3^4) table was employed to control the number of experiments and maintain representative results. Finally, artificial intelligence (AI) was introduced to simulate and optimize composite manufacturing. As shown in Table 1, four factors were recognized during preliminary study to produce relatively greater influence on physical and mechanical properties. They were labeled as F1 (the ratio of weight for bamboo flour to that of bamboo flour and HDPE), F2 (the ratio of weight for KH550 to that of bamboo flour), F3 (moulding temperature), and F4 (moulding time), for which their levels were referred to as L1, L2, and L3.

Table 1. L_9 (3^4) Orthogonal Experiment for Proposed Composite

Level \ Factor	F1 (wt%)	F2 (wt%)	F3 (°C)	F4 (min)
L1	70	2	140	8
L2	60	4	160	10
L3	50	6	180	12

Composite Fabrication

First, bamboo flour and plastic were dried in a 101-1AB electrothermal blowing box (Tianjin Taisite Co., Ltd, China). Then, bamboo was treated using silane solution and blended with HDPE in an SRH-10 high speed mixer (Beijing Zedao Co., Ltd, China). Next, the mixture was plasticized under the proper temperature and shear force in an SHJ co-rotating twin-screw extruder (Nanjing Giant Co., Ltd, China). Afterwards, extrudate was pelletized using a PC-180 strong plastic crusher (Dongguan Huangjiangdatian Co., Ltd, China). Finally, grains were assembled and moulded using a BY302×2/15 150T universal experimental press (Suzhou Xinxieli Co., Ltd, China).

Analytical Method

Crystalline and functional groups of virgin and 6 wt% KH550 treated bamboo flour was compared using XRD and FT-IR. The morphological/thermal properties of composite with 9 mm thickness made from bamboo (50 wt%) and KH550 (0 wt% and 6 wt%) under moulding parameters (180 °C and 12 min) were compared using SEM and DSC. The bamboo content and KH550 dosage were calculated consistent with the definition of F1 and F2 in Table 1.

Crystalline structure

Bamboo flour was pressed into slices. Then it was examined through an XRD-6000 diffractometer (Shimadzu, Japan). With Cu Kα radiation, a voltage of 40.0 kV, and a current of 30 mA, corresponding intensity curves were recorded from 3° to 40° (2θ) at a speed of 2 °/min.

Functional group

Bamboo flour blended with KBr powder was ground in agate mortars, pressed into sheets, and then scanned applying a Nicolet 5700 spectrometer to collect transmittance over the wavenumber of 4000 to 500 cm^{-1}.

Microscopic morphology

After freezing in liquid nitrogen, a 3 to 4 mm tensile fracture surface of composite was taken and coated with a thin layer of platinum in a vacuum, whose bottom was polished and fixed using conductive adhesive. At an accelerating voltage of 10.0 kV, the composite was observed under an S-3400N microscope (Hitachi, Japan).

Thermal stability

After being ground into powder, 3 mg of composite was taken and analyzed using a Netzsch-204 calorimeter (Netzsch, Germany). At a speed of 10 °C/min, data was collected from 40 °C to 200 °C.

Physical and mechanical properties

Considering potential application, R1 flexural strength (MPa), R2 flexural modulus (GPa), R3 tensile strength (MPa), R4 impact toughness ($kJ \cdot m^{-2}$), and R5 thickness swelling after 24 h water adsorption (%) were measured. This was to evaluate the proposed composite according to Chinese national standards GB/T 1449-2005 (flexural), GB/T 1447-2005 (tensile), GB/T 1451-2005 (impact), and GB/T 17657-2013 (swelling). In terms of GB/T 1446-2005, all the specimens were tested at temperature 23 °C and relative humidity 50%, while experiments were repeated ≥3 times to reduce the relative standard deviation to within 5%. A 5848 universal material testing machine (Instron, USA), AG-IC electronic mechanical testing machine (Shimadzu, Japan), ZBC1400-A pendulum impact testing machine (MTS, USA), and HH-W600 digital display water tank (Jintan Kexi Co., Ltd, China) were employed in this pursuit.

RESULTS AND DISCUSSION

Key Parameters in Composite Technology Route

Through trial and error, a roadmap for composites with a 50 to 70% higher bamboo plastic content ratio was obtained, as generalized in Fig. 1, while key parameters for important stages were also determined. This route consisted of three major steps. The first was pretreatment to remove excess water and extract that would produce vapor on the fiber surface and compromise adhesion in the composite interface; bamboo flour was heated to temperatures of 105 °C for about 8 h, until the moisture content decreased from around 8 to 10% to below 3%. Next, silane KH550 was diluted in ethanol to 1 wt%, hydrolyzed, and mixed well with dried bamboo flour for 20 min. Modified bamboo flour was then fully blended with dried HDPE for 10 min. The next step was granulation; at an engine speed of 20 r/min and a feeding speed of 12 r/min in extruder, the bamboo plastic mixture was further dried, dispersed, and plasticized to eliminate residual moisture and volatile substances. This process concerned bamboo content with ratios of engine and feeding speeds in the currently acceptable 1.5 to 2 range, thus avoiding locking and inefficiency once this value became higher or lower, respectively. Considering bamboo pyrolysis and HDPE melting, the temperature profile for five barrels was set at 80

°C→120 °C→135 °C→135 °C→130 °C to cause gradual melting of HDPE and to maintain a certain level of viscosity. After solidification, extrudate was pelletized into 1 to 3 mm flakes or granules to facilitate moulding, the final step. Assembly was carried out using hand lay-up techniques, while thickness (3 mm, 5 mm, 9 mm) was controlled in different steel moulds (300 mm × 300 mm, self-designed). Under 6 MPa pressure, hot pressing was performed according to orthogonal design, and cold pressing followed at room temperature for 3 min, thus harvesting the composite to be tested. The uniform mixture and fiber morphology were respectively affected by larger and smaller particle sizes of bamboo flour. As such, the results of this paper demonstrated that a mesh of 60 was an adequate level for composites applied in the engineering field.

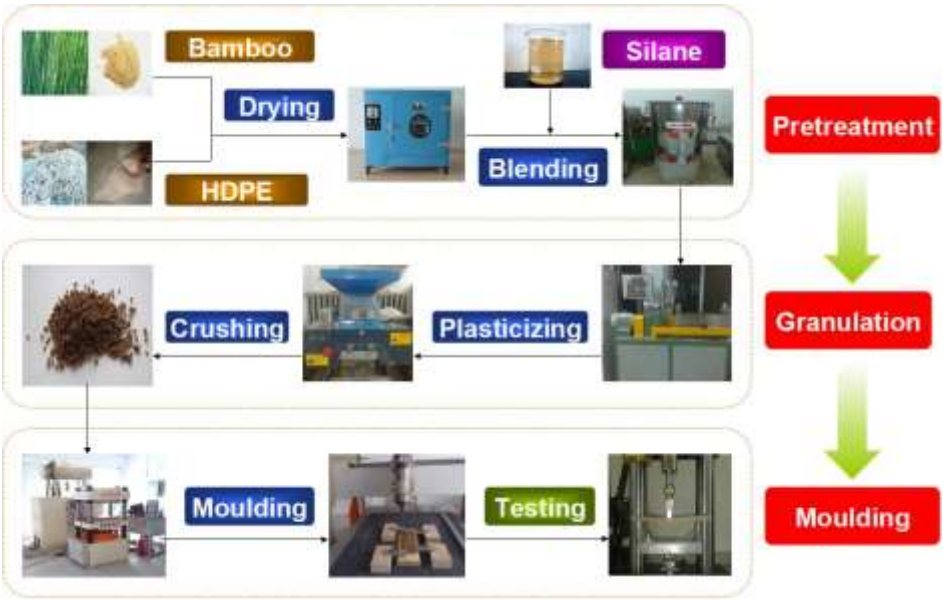

Fig. 1. Technological roadmap of proposed silane KH550 surface modified moso bamboo flour/HDPE composite engineering material

Characterization of Silane Modified Bamboo Plastic Interface

Crystalline structure and functional groups

Figure 2 displays an XRD graph for bamboo flour after being treating with 0% and 6% KH550. For both the modified and control sample, major sharp peaks always occurred at a 2θ value of around 16°, 22°, and 35°, which was caused by diffraction planes (101), (002), (040), and in accordance with the typical cellulose I polymorph (Zhao 2012; Lu *et al.* 2014; Wei *et al.* 2014). Overall, no evident variation was observed in position and shape of peaks, partly indicating that the crystal structure never changed, as the combination between silane and bamboo would not occur on cellulose. For one thing, because of the hydrogen bonds formed by intermolecular hydroxyl groups, bamboo cellulose often features relatively high crystallinity. The three-dimensional network structure and intermolecular force of lignin also diminish the accessibility of the reaction on cellulose (Chen *et al.* 2012). By virtue of XRD, X-ray photoelectron spectroscopy (XPS), and FT-IR, it has been demonstrated that the reaction of bamboo flour and silane KH560 takes place on the aldehyde group of lignin (Chen *et al.* 2012). In this context, the probable mechanism for bamboo flour and silane KH550 was deduced, and is shown in Fig. 3. Active $-OC_2H_5$ of silane KH550 first underwent hydrolysis in the presence of ethanol and water. The generated silanol featured a high affinity with natural fiber. Then,

a surface reaction subsequently occurred between the hydroxyl and aldehyde groups, while the silanol was grafted on the lignin surface.

After dehydration condensation, a -Si-O-Si- chain was further created, while the polarity of bamboo flour was greatly reduced. This process was different from silane A-171-modified poplar veneer, KH550-treated corn fiber, and KH560-modified bamboo cellulose, in which silanol is demonstrated to react with hydroxyl groups on cellulose (Fang *et al.* 2014; Lu *et al.* 2014; Luo *et al.* 2014). In general, the crystalline part of natural cellulose chains represents the most potential agents for reinforcing polymer (Ng *et al.* 2015). In the present work it was noticed that KH550 treatment led to a small increase in crystallinity (X_c) from 40.71 % to 41.82 %. This trend is similar to KH550-modified corn fiber/PLA composites, where X_c increases from 37.75 % to 41.49 %, as measured by DSC (Luo *et al.* 2014) The findings in this paper imply that the amorphous region on bamboo flour was partly destroyed during silane sizing, while new crystalline areas were harvested after rearrangement among macromolecular chains (Zhao 2012; Wei *et al.* 2014).

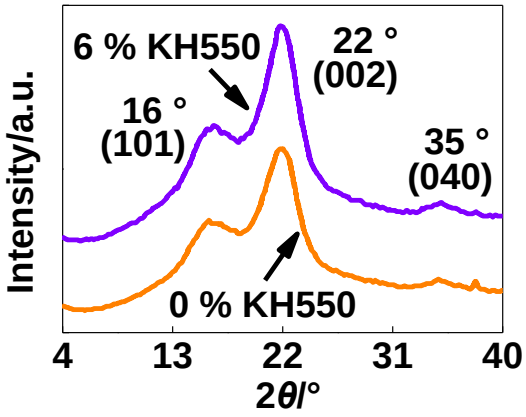

Fig. 2. XRD graph of KH550 surface modified moso bamboo flour and control sample

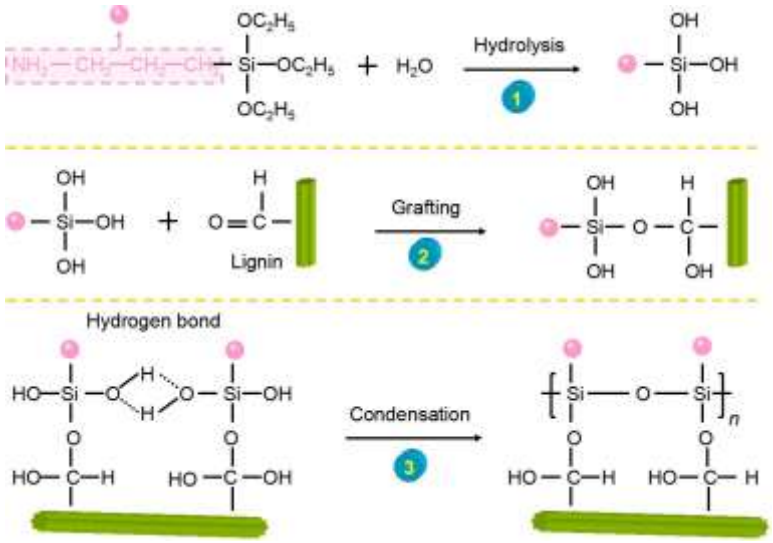

Fig. 3. Compatibilizing mechanism of KH550 on bamboo flour

In addition, some impurities with lower crystallinity were also removed from fibers during modification (Lu *et al.* 2014). Typically, the filler would simultaneously contribute to nucleating (increasing X_c) and exhibit a hindrance to migration and diffusion of polymeric molecular chains (decreasing X_c), which are two competing factors that dominate the crystallization process within a composite system (Luo *et al.* 2014). In this sense, modified bamboo flour with better interfacial compatibility would be more beneficial to the arrangement of an HDPE chain, resulting in a higher X_c for the composite.

To provide some more direct evidence with respect to the compatibilizing process, FT-IR was also employed for revealing the reaction mechanism between lignin and silane. As illustrated in Fig. 4, the spectrum of modified sample looked roughly like that of the control group, but several fingerprint regions still deserved attention, especially three peaks of most interest to this study. On one hand, enhanced intensity near 2900 cm^{-1} and 1100 cm^{-1} after modification would be respectively assigned to stretching vibrations of C-H and Si-O-C (Fang *et al.* 2014; Lu *et al.* 2014), in which the former would be raised by adding KH550 while the latter would be formed *via* reaction with silanol, thus proving the introduction of silane and occurrence of grafting. On the other hand, diminished intensity around 1700 cm^{-1} for modified sample would be an indication of lignin aldehyde carbonyl C=O stretching vibration (Luo *et al.* 2014), which would be concerned with decreased concentration due to grafting behavior, thereby further explaining the reaction site. Consequently, bamboo and KH550 would interact on the aldehyde group of lignin, thus achieving the compatibilization.

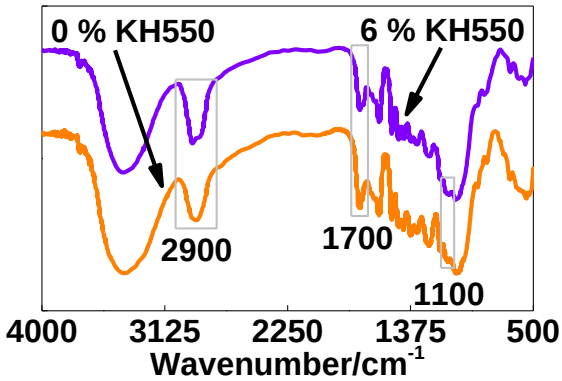

Fig. 4. FT-IR spectra of KH550 surface modified moso bamboo flour and control sample

Microscopic morphology

Figure 5 exhibits the SEM image of the tensile fracture surface containing 0% and 6% KH550 for the composite. As illustrated, composites featured highly porous surfaces with interpenetration between bamboo flour fiber and the HDPE network. It was apparent that plenty of natural fibers acted as a reinforcing phase for the plastic and played a key role with respect to mechanical behaviors (Abdul Khalil *et al.* 2012; Zakikhani *et al.* 2014). Nevertheless, marked change at the interface could be recognized. For the control group, broken fibers presented smooth surfaces and loose distributions, and they failed to be embedded in resin due to relatively poor wettability. There was a clear gap between fiber and polymer, as adequate interfacial interaction never formed. In contrast, the modified sample included fractured fibers that showed a rougher surface and tight array, and were deeply surrounded by the matrix with melting HDPE clearly coated on the fibers' surface. In addition, the fracture surface was relatively irregular, with a more

intricate interlocking occurring between the two phases. Overall, introduction of silane made a difference for the bamboo plastic system, especially in their dispersion, thus facilitating effective stress transmitting along the interface (Lu *et al.* 2014). It should be noted that the improvement effect of silane KH550 on composite morphology in this case was consistent with KH550 on rice husk/PP, KH550 on corn fiber/PLA, and KH560 treated bamboo cellulose/PLLA composite (Lu *et al.* 2014; Luo *et al.* 2014; Yeh *et al.* 2015).

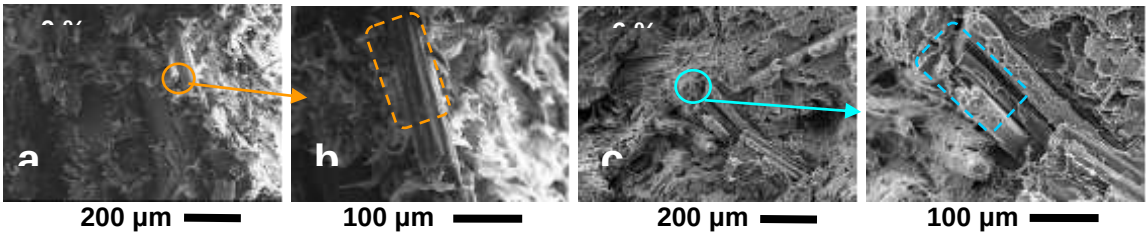

Fig. 5. SEM image of tensile fracture surface of KH550 compatibilized composite and control sample

Thermal stability

Heat endurance serves as an important reflection of interfacial compatibility (Li *et al.* 2014; Lei *et al.* 2015; Yeh *et al.* 2015). Figure 6 depicts DSC curves of bamboo plastic composite with 0% and 6% KH550 additions. When an endothermic phenomenon occurred, there was a bulge in the profile that indicated the melting temperature (T_m) of the materials, which is concerned with transformation between the solid and liquid phase (Luo *et al.* 2014). Generally speaking, a higher T_m implies that segments of the polymer were more hindered by its circumstance (Lu *et al.* 2014). As seen, T_m of the sample was elevated while the peak area also increased after silane treatment, leading to an improved thermal stability of the composite. For example, T_m and melting enthalpy (ΔH_m) of the control sample were 128.46 °C and 34.61 J/g, respectively. This is remarkably lower than the 131 °C T_m value of pure HDPE. However, the modified composite displayed marked improvement with T_m 130.83 °C and ΔH_m 39.88 J/g. This was mainly ascribed to a better hindrance effect of the KH550 surface treated bamboo flour provided by enhanced fiber stiffness, and interaction with the matrix (Luo *et al.* 2014). Since T_m would be decreased once some resin molecules were degraded into smaller ones and served as a plasticizer (Lu *et al.* 2014), it was also demonstrated that decomposition of HDPE never occurred during silane coupling modification. In a word, it was confirmed that modification facilitated mutual wettability and penetration of natural fiber and the polymer matrix, while greater intermolecular forces restricted chain segment movement, thus boosting interfacial compatibility (Zhao 2012). Similar reports on other materials can be found too. For example, T_g (glass transition temperature, another indicator of thermal stability related to change from glass to a rubbery state) of bamboo cellulose/PLLA composite is slightly promoted using KH560, at which segments of resin start to move (Lu *et al.* 2014). Additionally, KH550 can increase T_g and ΔH_m of corn fiber/PLA composites from 47.5 °C to 57.4 °C and 28.3 J/g to 31.1 J/g, while its heat distortion temperature (HDT) and crystallization temperature (T_c) are also significantly heightened from 55.5 °C to 60.1 °C and from 103.0 °C to 114.9 °C (Luo *et al.* 2014).

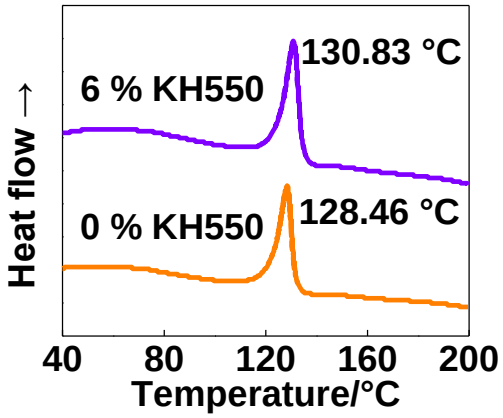

Fig. 6. DSC curve of KH550 compatibilized composite and control sample

Effect of Process on Composite Physical and Mechanical Properties

Effect of thickness

Since moso bamboo flour/KH550/HDPE has been confirmed to be a feasible combination for developing novel biocomposites, the effect of processes on this combination should be investigated. In practice, thickness would be an important parameter concerned with application. Figure 7 presents the statistical result of physical and mechanical properties for 3 mm, 5 mm, and 9 mm composites. As can be seen, with the increase in thickness, five properties were improved overall. From 3 to 5 mm, R2 (flexural modulus) and R5 (thickness swelling) were greatly promoted, R3 (tensile strength) and R4 (impact toughness) were slightly boosted, and R1 (flexural strength) varied relatively little. From 5 to 9 mm, all the mechanical properties were obviously enhanced, while R5 showed less change.

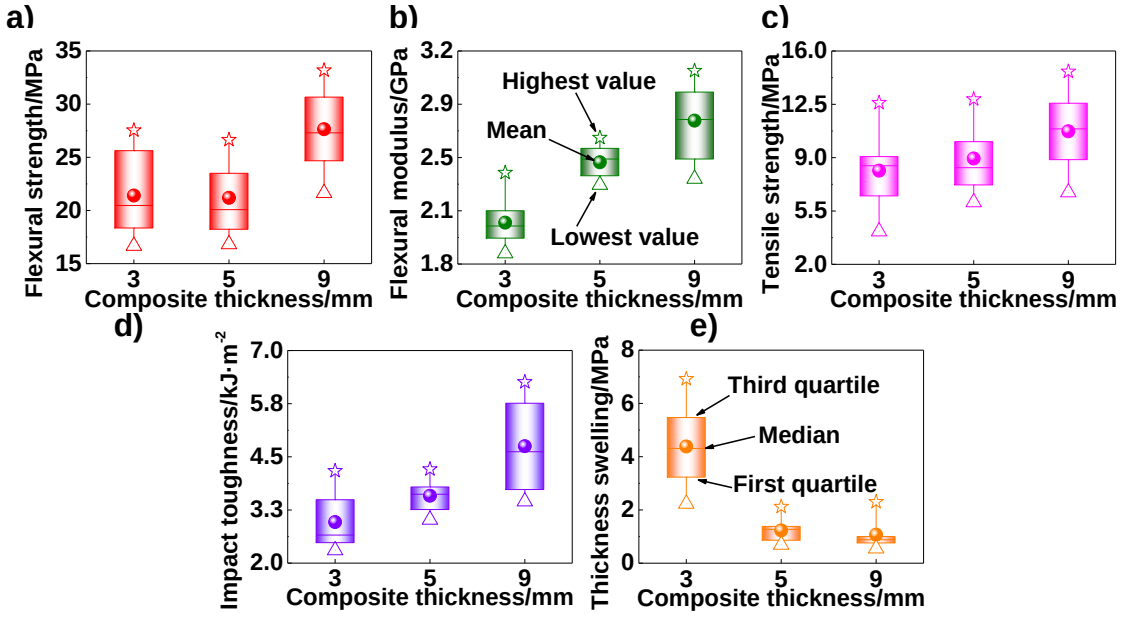

Fig. 7. Influence of composite thickness on physical and mechanical properties

Generally speaking, lower thickness would contribute to the full reaction during composite preparation, especially moulding, resulting in better physical and mechanical properties. For instance, R1, R2, and R5 are also specified in GB/T 17118-2009

"Medium density fiberboard (MDF)", whose thickness is divided into several ranges among 1.5 mm, 3.5 mm, 6 mm, 9 mm, 13 mm, 22 mm, and 34 mm. The thinner MDF is, the stricter the requirement becomes. In this context, the current trend seemed to be an abnormal phenomenon. In fact, a similar variation of R2 and R3 against thickness can also be observed in poplar/HDPE plywood (Fang *et al.* 2013a). Consequently, the present result would be connected with different interface interactions between wood-based panel and fiber reinforced thermoplastic (Lei *et al.* 2015; Yeh *et al.* 2015).

Effect of material and moulding parameters

As indicated by Fig. 8, variance analysis revealed that F1 and F2 would be the most significant factors affecting R1 to R5 (while F1>F2). Figures 8 through 10 were provided to further recognize the effect of F1 to F4 on composites with different thickness. For (a) and (b) of the range analysis, range was respectively categorized by independent (F1 to F4), and dependent variables (R1 to R5) to highlight the "influence of factor" and "sensitivity of result". For (c) through (f), the average of the property at a level was calculated to explore the relation between material performance and factor level. For convenience, all data were normalized by dividing the corresponding (thickness) maximum value in the orthogonal experiment.

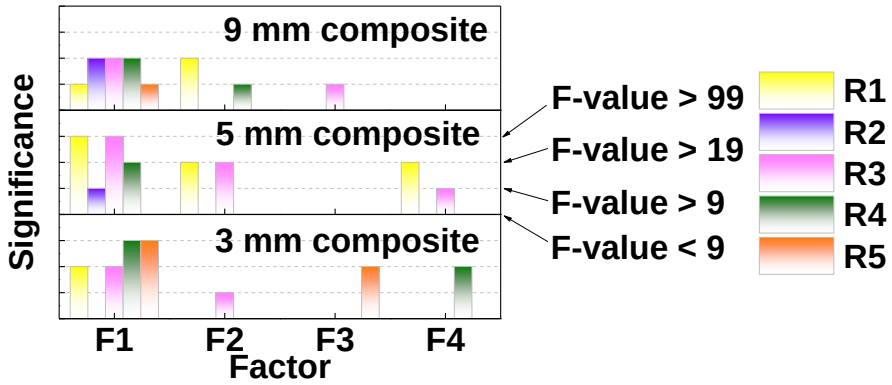

Fig. 8. Variance analysis of material and moulding parameters on physical and mechanical properties. F1: bamboo content (wt%), F2: KH550 dosage (wt%), F3: moulding temperature (°C), F4: moulding time (min); R1: flexural strength (MPa), R2: flexural modulus (GPa), R3: tensile strength (MPa), R4: impact toughness (kJ·m^{-2}), R5: thickness swelling (%)

As can be seen for the 3 mm composite (Fig. 9), F1 (bamboo content) presented >30% influence on R1 and R3 to R5 while F2 (modifier content), F3 (moulding temperature), and F4 (moulding temperature) respectively had >10% impact on R3, R5, and R4. On the other hand, R1 to R5 exhibited similar sensitivities to F1 through F4, in that all of them were very susceptible to F1, except for R2. For 5 mm composite (Fig. 10), both F1 and F2 produced >10% influence on 3 to 4 results, while both F3 and F4 had >10% impact on R5; F1 still had the greatest effect. Furthermore, R5 was very susceptible to F1-F4. The outcomes R1, R3, and R4 were relatively vulnerable to F1, and the sensitivity of R2 could almost be negligible. For 9 mm composite (Fig. 11), F1 generated >10% influence on all the data, in which three of them were over 30%. F2, F3, and F4 respectively resulted in >10% impact on 3, 2, and 1 performances. Like the 5 mm composite, R5 was very sensitive to F1-F4, while R1-R4 were susceptible to up to 2 factors. For every thickness, F1 was most influential, while R5 was most susceptible. With the rise of F1 to F4 levels, R1 to R5 were improved overall, but their optimal values

did not appear at a fixed level. Moreover, it should be pointed out that a higher F1 was prone to markedly compromise impact toughness (R4) and water resistance (R5), which was opposite to its effects on R1 through R3.

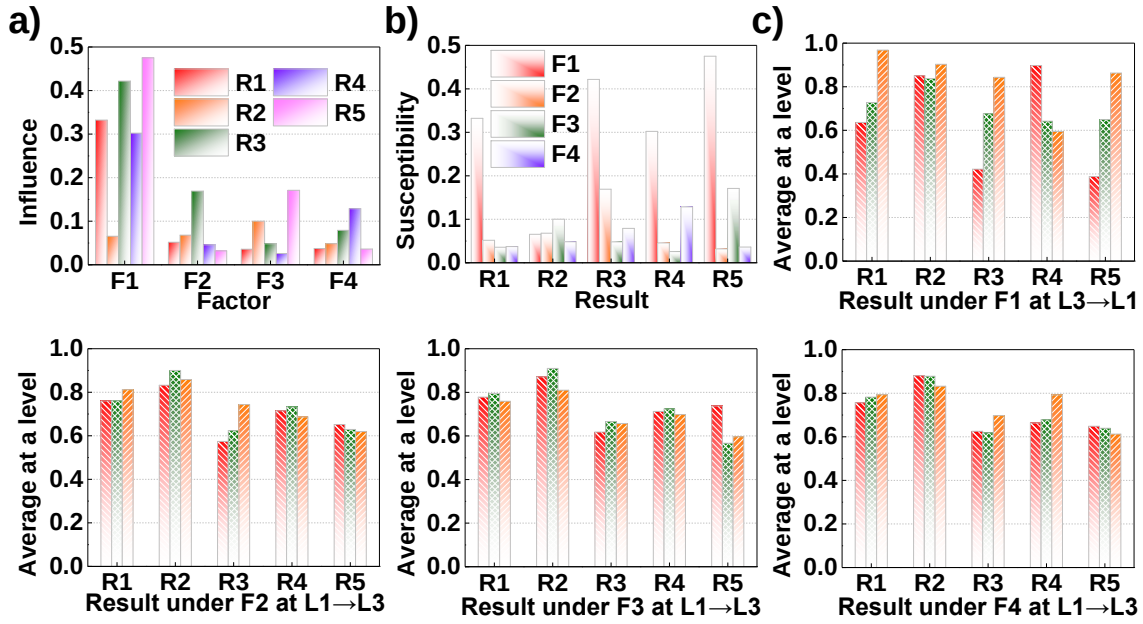

Fig. 9. Interaction between material, moulding parameters, and physical/mechanical properties of 3 mm composite. F1: bamboo content (wt%), F2: KH550 dosage (wt%), F3: moulding temperature (°C), F4: moulding time (min); R1: flexural strength (MPa), R2: flexural modulus (GPa), R3: tensile strength (MPa), R4: impact toughness (kJ·m^{-2}), R5: thickness swelling (%)

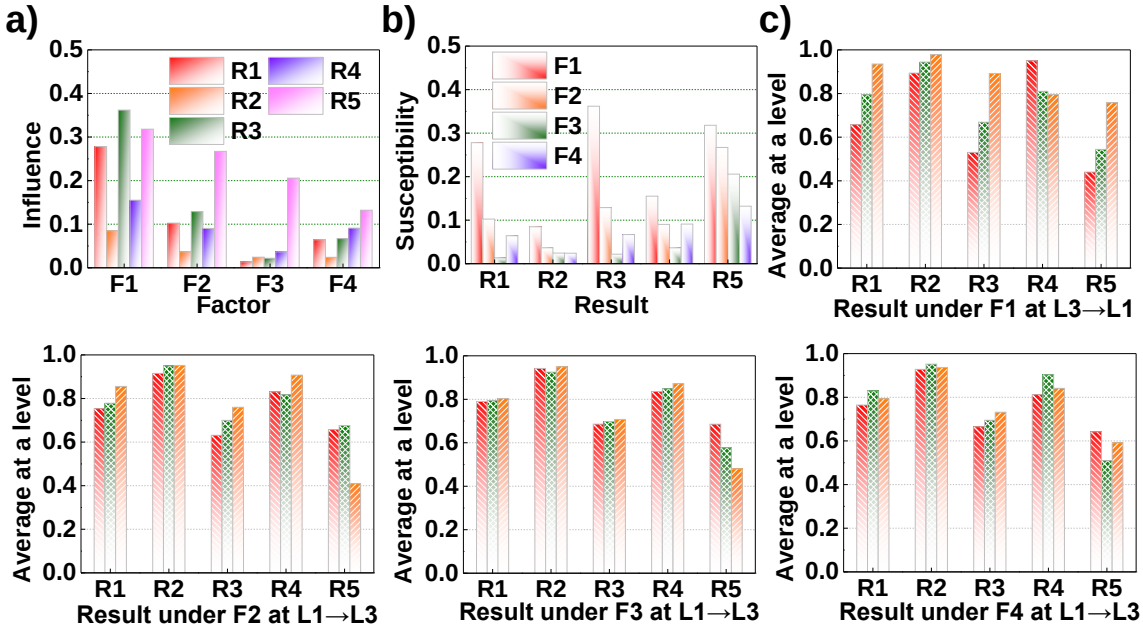

Fig. 10. Interaction between material, moulding parameters, and physical/mechanical properties of 5 mm composite. F1: bamboo content (wt%), F2: KH550 dosage (wt%), F3: moulding temperature (°C), F4: moulding time (min); R1: flexural strength (MPa), R2: flexural modulus (GPa), R3: tensile strength (MPa), R4: impact toughness (kJ·m^{-2}), R5: thickness swelling (%)

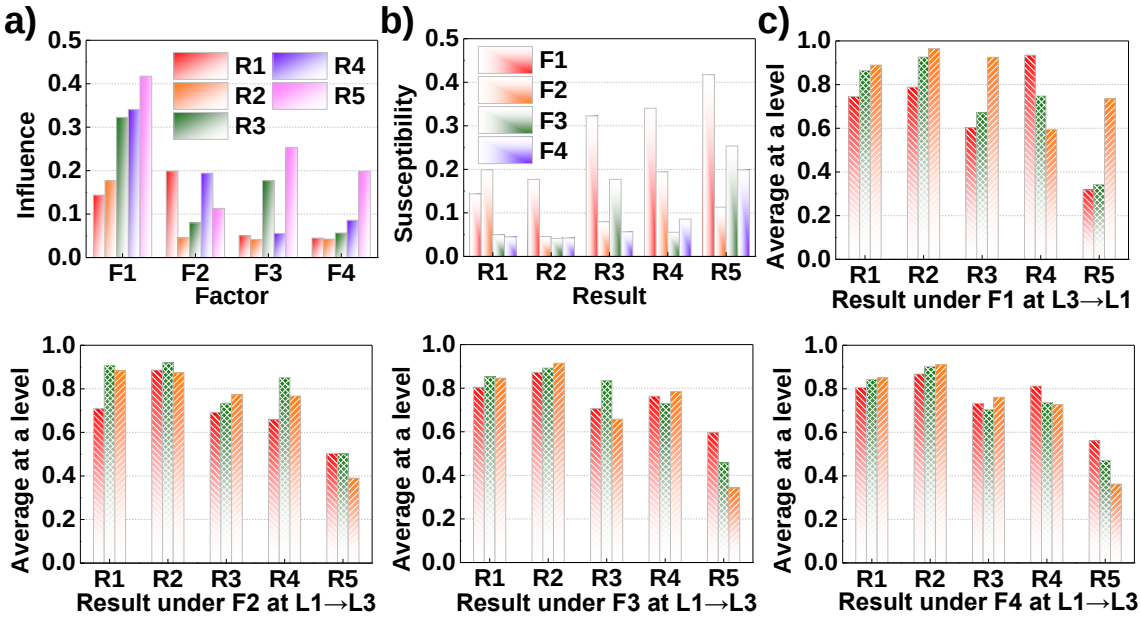

Fig. 11. Interaction between material, moulding parameters, and physical/mechanical properties of 9 mm composite. F1: bamboo content (wt%), F2: KH550 dosage (wt%), F3: moulding temperature (°C), F4: moulding time (min); R1: flexural strength (MPa), R2: flexural modulus (GPa), R3: tensile strength (MPa), R4: impact toughness (kJ·m^{-2}), R5: thickness swelling (%)

The above results are understandable as follows. For one thing, the content of bamboo flour posed the greatest impacts on various performances, which agreed well with previous reports. As a rigid substance, fibers within bamboo flour are typically stiff and do not bend, stretch, or twist easily, which can remarkably heighten flexural and tensile properties of polymer (Wang *et al.* 2014; Cheng *et al.* 2015). For instance, with 30 wt% bamboo pulp fiber, PP composite possesses a greater flexural strength of 18→30 MPa, and tensile strength of 20→45 MPa, when its flexural modulus is increased even by 586.79% (Ren *et al.* 2014). On the other hand, due to the lack of flexibility, addition of natural fiber would also undermine the impact toughness of a composite (Zhao 2012). For example, with an increase of rice husk around 0 to 50 wt%, the impact strength of PP composite decreases by over 50% (Yeh *et al.* 2015). Similar variation can be found in bamboo cellulose/PLLA and corn fiber/PLA composite (Lu *et al.* 2014; Luo *et al.* 2014). However, it should be noted that an excess loading of natural fiber would also diminish flexural and tensile performances due to inefficient stress transfer caused by filler agglomeration, which leaves plenty of holes within the composite and decreases the contact area between the reinforcement and the matrix (Lei *et al.* 2015). In contrast to HDPE, bamboo flour is composed of polyhydroxy natural polymer, and it features highly hydrophilic character due to plenty of lignocellulose, which must significantly affect the water or moisture absorption behavior of its polymer composite (Li *et al.* 2013; Li *et al.* 2014; Wang *et al.* 2014; Lei *et al.* 2015; Yeh *et al.* 2015). For example, under a mechanism of general Fickian diffusion, it is found that the moisture diffusion coefficient (D_m) of bamboo fiber/HDPE composite would be in the range of 0.115×10^{-8} to 1.267×10^{-8} cm^2/s. This rises with the increase of a fiber loading level from 10 to 40 wt%. In this sense, natural fiber would undergo swelling or shrinking processes after water uptake and drying, during which adhesion damage with the matrix can be caused (Du *et al.* 2014).

Then, poor interfacial bonding may compromise other mechanical properties too, which should be taken seriously (Zakikhani *et al.* 2014). Similar effects on water and moisture adsorption can also be observed in poplar/HDPE plywood (Fang *et al.* 2013a). To enhance the impact ductility and moisture resistance, approaches such as adding plasticizer and heat treatment can be respectively considered during composite fabrication (Du *et al.* 2014; Xie *et al.* 2014).

For another, the positive role of silane KH550 in a bamboo plastic system has been examined using XRD, SEM, and DSC in this paper. Many investigations confirm that there would be a critical dosage of compatibilizer in composite, thus creating optimal performance (Yeh *et al.* 2014). For example, corn fiber/PLA composite, modified using 12 wt% KH550, shows better flexural and tensile properties than both 8 wt% and 16 wt% (Luo *et al.* 2014). Bamboo fiber/PLA composite treated with 15 wt% PLA grafting GMA obtains the best tensile and impact properties within the range 0 to 25 wt% (Wang *et al.* 2014). Since the optimal level of KH550 for proposed composite was not very obvious, artificial intelligence (AI) was subsequently introduced to determine this value.

Furthermore, a high enough moulding temperature and time are necessary to result in a more effective interaction between the reinforcement and matrix, as well as in the formation of their bonded joints (Fang *et al.* 2013b). Within a suitable range, a relatively high temperature and length of time helped the thermoplastic material to fully melt, disperse, and penetrate amid the plant unit, thus achieving better physical and mechanical properties. However, it should be pointed out that a higher temperature and length of time also increases the likelihood of bamboo flour carbonization, and coupling agent pyrolysis, leading to a waste of material and energy (Zhao 2012). In this paper, moulding condition was adequate overall, but optimal parameters should be analyzed with an algorithm similar to that used here for modifier dosage.

Application analysis of experimental data

To date, wood based panels (*e.g.*, fiberboard, particleboard, blockboard, and plywood) still play a key role in the furniture and construction industries. With extensive use of formaldehyde adhesive, organic emissions are known to pose an extraordinary threat to the environment and human health. Considering the similar type of plant unit, if the proposed formaldehyde-free biocomposite can serve as a feasible substitute for fiberboard, huge economic, social, and ecological benefits will be harvested. Taking commonly-used MDF as an example, Fig. 12 compares R1, R2, and R5 of the orthogonal experiment to corresponding requirements specified in GB/T 17118 "MDF". This categorizes MDF into load-bearing (construction material), furniture grade (decoration material), and general purpose (other application), with high, medium, and low demands, while the value on the thin (1.5 to 3.5 mm) is stricter than the medium (3.5 to 6 mm) and thick (6 to 9 mm) specimens. To clarify, just the requirements that promise to be reached were given using line sin Fig. 11. For flexural strength, condition 3 for 3 mm and 5 mm composites, and conditions 2, 3, 5, 6, 8, and 9 for 9 mm composites could meet the needs of general purpose. Conditions 2, 3, 5, 6, and 9 for 9 mm composites were better than the required furniture grade as well. For flexural modulus, conditions 2 and 3 for 5 mm composites, and 1 to 6 for 9 mm composites could simultaneously meet the needs for general purpose and furniture grade. Conditions 1, 2, and 5 for 9 mm composites were also in excess of load-bearing requirements. For thickness swelling, it was evident that all the results were much better than the standards, thus demonstrating excellent dimensional stability. By and large, condition 3 for 5 mm composites, and conditions 2, 3, 5, and 6 for

9 mm composites could serve as general purpose MDF, with the latter also applying to furniture grade.

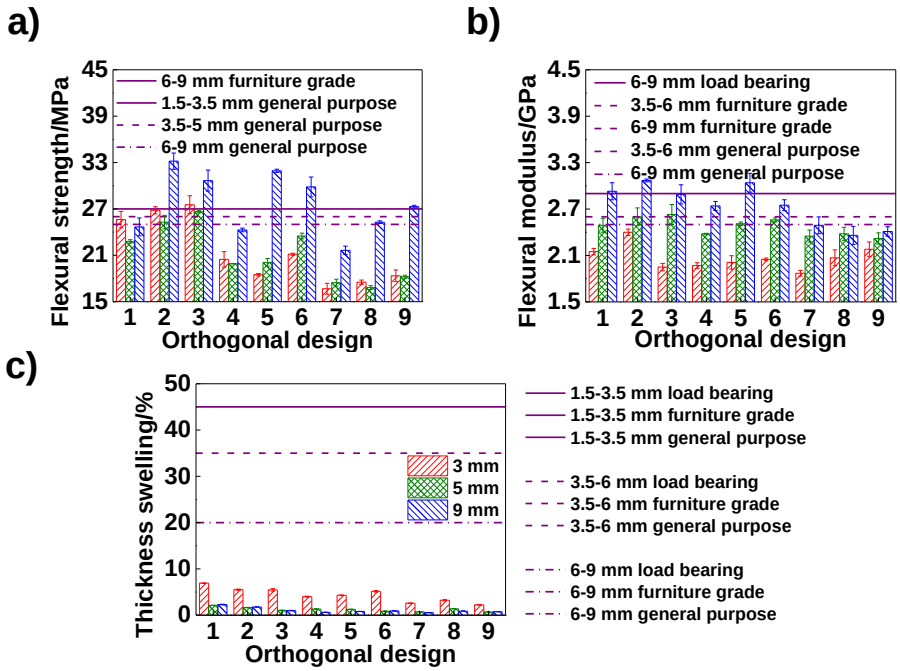

Fig. 12. Comparison of orthogonal experiment data of proposed composite with corresponding requirements in GB/T 17118 "MDF"

Optimal Fabrication Based on Artificial Intelligence (AI) Simulation

Model development

As a popular methodology in many fields, an artificial neural network (ANN) approach has been found to be more convenient when dealing with multi-objective optimization, compared to the response surface method (RSM) or support vector machine (SVM) (Yildirim *et al.* 2011; Özşahin 2012; Zainuddin *et al.* 2012; Fang *et al.* 2013b; Chiranjeevi *et al.* 2014; Emeko *et al.* 2015). Since 9 mm composites possessed better physical and mechanical properties, ANN was employed to further explore its feasibility in construction applications. MATLAB 7.0 language (MathWorks, USA) was adopted to perform the technical computing. Figure 13 presents a typical feed-forward back-propagation ANN topology describing composite preparation, with architecture consisting of three layers containing many neurons. In detail, neurons of input and output layers respectively indicated factors F1-F4, and results R1-R5, with fourteen neurons finally taken for a hidden layer after trial and error. Between neighboring layers, every neuron of the former was connected to that of the latter. For hidden and output layers, neurons served as some information processing centers (Yildirim *et al.* 2011), that gathered and adjusted intricate signals as follows (Eq. 1),

$$y_j = f\left(\sum_{i=1}^{k} x_i \cdot w_{i\to j} + \theta_j\right) \quad (1)$$

where x_i is the input signal from neuron i to neuron j, $w_{i\to j}$ is the weight between two junctions, k is the number of neurons in the former layer, θ_j is the threshold that belongs to neuron j, f is the transfer function between two layers, and y_j is the output of neuron j.

Typically, hyperbolic tangent sigmoid (TANSIG) and linear (PURELIN) functions would respectively be used for input-hidden, and hidden-output layers (Özahin 2012).

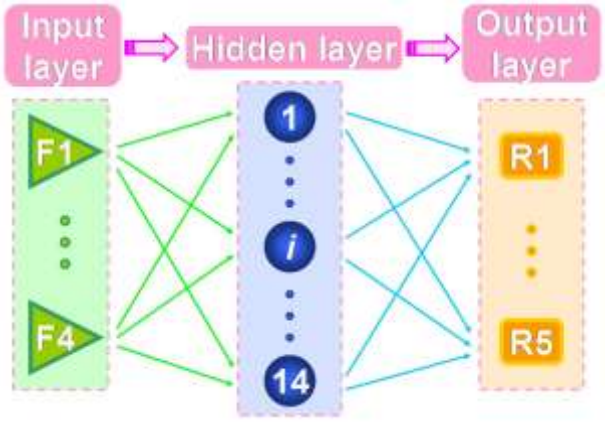

Fig. 13. Artificial neural network for the association between process and performance of proposed composite. F1: bamboo content (wt%), F2: KH550 dosage (wt%), F3: moulding temperature (°C), F4: moulding time (min); R1: flexural strength (MPa), R2: flexural modulus (GPa), R3: tensile strength (MPa), R4: impact toughness (kJ·m^{-2}), R5: thickness swelling (%)

Network training and experimental validation

Due to uniform dispersion and neat comparability, both number and representativeness of the orthogonal experiment were adequate for training the initial ANN, which contributed to recognizing the general mapping rule, and avoiding the over-fitting caused by excess input. To accelerate convergence and reduce error during machine learning, input was converted from -1 to 1 (Chiranjeevi *et al.* 2014) according to Eq. (2), while an inverse transform was applied to output,

$$z' = 2 \times \frac{z - z_{min}}{z_{max} - z_{min}} - 1 \quad (2)$$

where z is the experimental result, z_{max} and z_{min} are the maximum and minimum values of z, and z' is the corresponding dimensionless signal. Applying the Levenberg-Marquardt (L-M) algorithm, data were first entered in the input layer, flowed through a hidden layer, and finally arrived at an output layer. During this process, the weight and threshold were randomly generated initially, and continually modified in compliance with the given convergence criteria (*i.e.*, epochs=3000 and error goal<10^{-14} in this paper), thus achieving optimal similarity between calculation and observation. Subsequently, robustness of ANN was evaluated from two aspects: reproduction and prediction abilities (Emeko *et al.* 2015). For the former, the network was trained by all the data. Then, R1-R5 under 9 conditions were computed, and compared with experiments. As illustrated in Fig. 14, simulation was concentrated near $y=x$, and scatters were never found, in which coefficients of determination (R^2) for R1-R5 were 1 while relative error was negligible, thus demonstrating the reproductive capability of ANN. For the latter, a cross validation was necessary. In other words, data of conditions 1 to 4, 6 to 9, and condition 5, served as training and testing sets to verify whether a general mapping rule could be acquired by ANN. As displayed in Fig. 15, the consistence was satisfactory overall, with most results giving deviations lower than 10%, while the maximum value was just 13.74% for R2, thus validating the predictive capability of ANN.

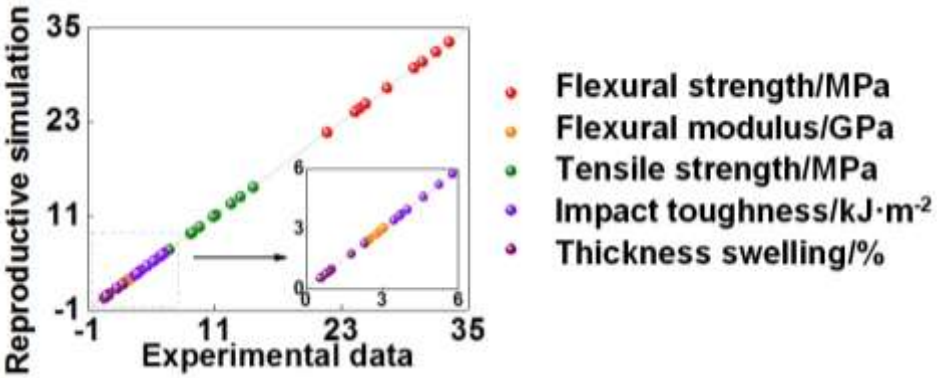

Fig. 14. Validation of the reproductive capability of ANN

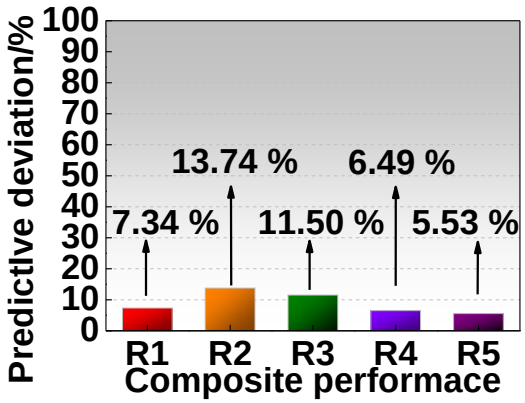

Fig. 15. Validation of the predictive capability of ANN. R1: flexural strength (MPa), R2: flexural modulus (GPa), R3: tensile strength (MPa), R4: impact toughness (kJ·m^{-2}), R5: thickness swelling (%)

ANN Optimization and experimental validation

By virtue of ANN, R1 through R5 under any condition can be predicted, and adequate combinations of F1-F4 that produce better performances can be sought (Zainuddin *et al.* 2012). Considering that, a detailed numerical experiment was conducted with five levels set by average in the original range of F1-F4. In other words, levels of F1 (bamboo content) included 50, 55, 60, 65, and 70 wt%. Levels of F2 (KH550 dosage) involved 2, 3, 4, 5, and 6 wt%. Levels of F3 (moulding temperature) included 140, 150, 160, 170, and 180 °C. Levels of F4 (moulding time) contained 8, 9, 10, 11, and 12 min. On the other hand, 625 conditions were considered during this simulation, in which levels of F1-F4 were updated every 125, 25, 5, and 1 times, respectively. Figure 16 presents interesting results of the simulation, in which requirements of R1, R2, and R5 for load-bearing MDF listed in GB/T 17118 are marked. As shown, there were always several R1s over the standard line every 125 times, with higher outcomes of R2 concentrated in conditions 375-625. All the values were far better than the limit for R5. Moreover, R1 featured a regular rise and fall amid a similar range every 125 times, implying a stronger interaction with F2, which also completed a cycle every 125 times. In contrast, an evident increase of R2, R3, and R5, as well as a remarkable decrease of R4, could be observed every 125 times, indicating a greater susceptibility to F1 that also updated every 125 times. Clearly, these discoveries agreed well with those demonstrated in Fig. 11, partly validating this model again.

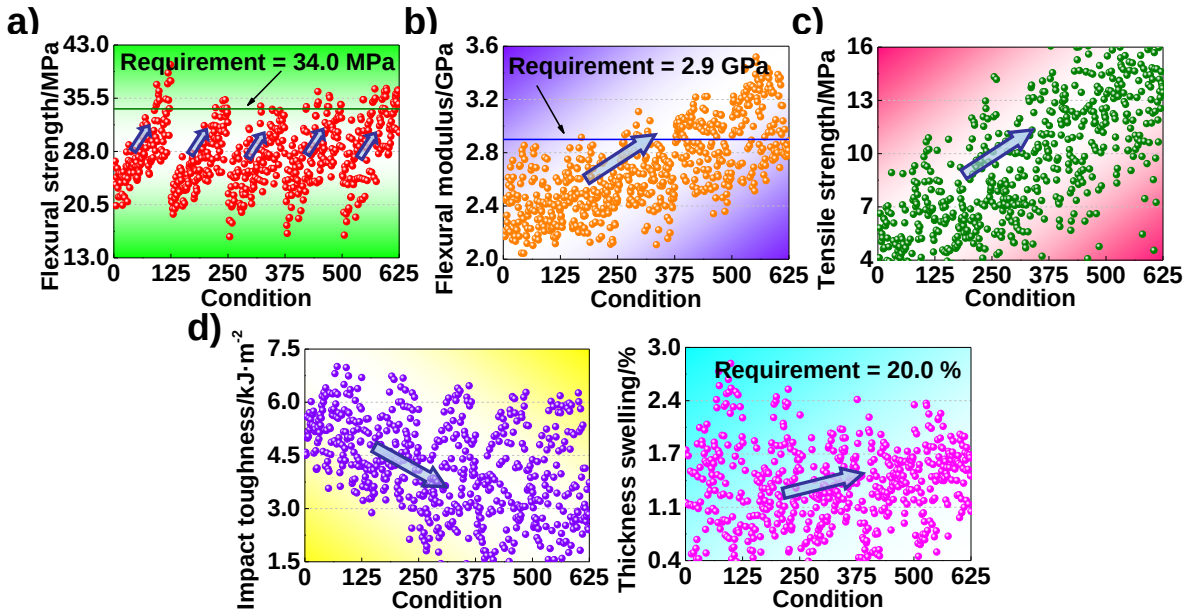

Fig. 16. ANN numerical experiments of composite performance at 625 conditions

Overall, 12 combinations of F1-F4 that met the comprehensive demands of load-bearing MDF (R1=34.0 MPa, R2=2.9 GPa, and R5=20.0 %) could be selected, thus forming a solution set. Since a greater R1-R4 (R1: flexural strength, R2: flexural modulus, R3: tensile strength, R4: impact toughness) and a smaller R5 (thickness swelling) were desirable, a fitness function was proposed to further determine an optimal process from the global perspective (Eq. 3):

$$\text{fitness} = \prod_{i=1}^{4} R i \Big/ R 5 \quad (3)$$

Overall, the fitness was in the range of 2000 to 9000, while F1=65 wt%, F2=3 wt%, F3=180 °C, F4=9 min, and F1=70 wt%, F2=3 wt%, F3=180 °C, F4=8 min respectively provided the minimum 2118, and maximum 8496 (F1: bamboo content, F2: KH550 dosage, F3: moulding temperature, F4: moulding time). Consequently, experiments were performed three times under the latter to validate current predictions, and yielded R1=37.16±0.84 MPa, R2=3.62±0.15 GPa, R3=14.02±0.25 MPa, R4=6.28±0.22 kJ·m^{-2}, and R5=1.14±0.02 %, in which all the deviations between simulation and observation were less than 10%. These results demonstrated the effectiveness of AI optimization and also revealed the potential of the proposed bamboo-plastic composite in construction applications.

CONCLUSIONS

1. Based on the combination of moso bamboo flour-silane KH550-HDPE, a pretreatment/granulation/moulding technical route was proposed to manufacture composite engineering material with a higher bamboo plastic mass ratio, blazing a new trail for beneficial usage of forestry processing residue, as well as for minimizing pollution related to discarding of used plastics.

2. During surface modification, reactions between bamboo flour and KH550 took place on the aldehyde group of lignin.
3. After 6 wt% KH550 treatment, the crystallinity of bamboo increased from 40.71% to 41.82 %, while the melting temperature and enthalpy of composites rose from 128.46 °C and 34.61 J/g to 130.83 °C and 39.88 J/g. These compatibilization effects agreed with improved interface morphology.
4. With increasing in thickness from 3 to 9 mm, physical and mechanical properties of composite were improved overall. Bamboo content and moulding time respectively provided the greatest and weakest influences on performance, while thickness swelling and flexural modulus displayed the biggest and smallest sensitivities to the process, respectively.
5. Higher bamboo content improved flexural and tensile properties but diminished toughness and water resistance, while KH550 dosage moulding parameters presented complicated interactions with the performances.
6. Applying an ANN simulation, the association between process and performance was modeled and optimized, showing that a KH550 content of 3 wt%, a moulding temperature of 180 °C, and a time of 8 min made a 9 mm composite with 70 wt% bamboo can achieve a load bearing MDF level in GB/T 11718.
7. The present data supports the formation of a first "Bamboo Plastic Composite" standard proposed by the authors' team for the Chinese forestry industry, while future research would focus on enhancing ductility and dimensional stability, thus promoting comprehensive development.

ACKNOWLEDGMENTS

Hearty thanks are extended to the Beijing Co-built Project (2012) "Technology and Theory on Efficient Processing and Utilization of Wood Materials," Beijing Co-built Project (2014) "Manufacture and Application of Novel Wood Composites", Beijing Co-built Project (2010) "Research on Key Technology of Wood Efficient Utilization," and Zhejiang Chengzhu Co., Ltd. Co-built Project (2014-10) "Research and Application on Bamboo Composites and Environmentally Friendly Adhesives".

Besides, we are also deeply grateful to the Chinese Industry Standard Project (2013-LY-192) "Bamboo Plastic Composite", Beijing Natural Science Foundation (2122045) "Study on the Interfacial Bonding Mechanism of Bamboo Plastic Engineering Composites" and National Natural Science Foundation (3157030345) "Research on Reaction, Transfer and Control of Hazardous Plasticizer PAEs in Wood Plastic Composite and its Environmental Interface".

REFERENCES CITED

Abdul Khalil, H. P. S., Bhat, I. U. H., Jawaid, M., Zaidon, A., Hermawan, D., and Hadi, Y. S. (2012). "Bamboo fibre reinforced biocomposites: A review," *Mater. Design* 42, 353-368. DOI: 10.1016/j.matdes.2012.06.015

Chen, Q., Bai, W., Xu, Y., and Lin, J. (2012). "Chemical structure and reaction scheme of modified bamboo powder with silane coupling agent," *Chem. Ind. Forest Prod.* 32, 27-31.

Cheng, H., Gao, J., Wang, G., Shi, S. Q., Zhang, S., and Cai, L. (2015). "Enhancement of mechanical properties of composites made of calcium carbonate modified bamboo fibers and polypropylene," *Holzforschung* 69, 215-221. DOI: 10.1515/hf-2014-0020

Cheng, H., Gao, J., Wang, G., Shi, S. Q., Zhang, S., and Cai, L. (2014). "Effect of temperature on calcium carbonate deposition in situ on bamboo fiber and polymer interfaces," *Wood Fiber Sci.* 46, 247-258.

Chiranjeevi, P. V., Pandian, M. R., and Thadikamala, S. (2014). "Integration of artificial neural network modeling and genetic algorithm approach for enrichment of laccase production in solid state fermentation by *Pleurotus ostreatus*," *BioResources* 9, 2459-2470. DOI: 10.15376/biores.9.2.2459-2470

Correia, V. D. C., Santos, S. F., Mármol, G., Curvelo, A. A. D. S., and Savastano Jr., H. (2014). "Potential of bamboo organosolv pulp as a reinforcing element in fiber–cement materials," *Constr. Build. Mater.* 72, 65-71. DOI: 10.1016/j.conbuildmat.2014.09.005

Du, L., Li, Y., Lee, S., and Wu, Q. (2014). "Water absorption properties of heat-treated bamboo fiber and high density polyethylene composites," *BioResources* 9, 1189-1200. DOI: 10.15376/biores.9.1.1189-1200

Emeko, H. A., Olugbogi, A. O., and Betiku, E. (2015). "Appraisal of artificial neural network and response surface methodology in modeling and process variable optimization of cxalic acid production from cashew apple juice: A case of surface fermentation," *BioResources* 10, 2067-2082. DOI: 10.15376/biores.10.2.2067-2082

Fang, L., Chang, L., Guo, W., Chen, Y., and Wang, Z. (2014). "Influence of silane surface modification of veneer on interfacial adhesion of wood–plastic plywood," *Appl. Surf. Sci.* 288, 682-689. DOI: 10.1016/j.apsusc.2013.10.098

Fang, L., Chang, L., Guo, W., Ren, Y., and Wang, Z. (2013a). "Preparation and characterization of wood-plastic plywood bonded with high density polyethylene film," *Eur. J. Wood Prod.* 71, 739-746. DOI: 10.1007/s00107-013-0733-0

Fang, L., Chang, L., Guo, W., Chen, Y., and Wang, Z. (2013b). "Manufacture of environmentally friendly plywood bonded with plastic film," *Forest Prod. J.* 63, 283-287. DOI: 10.13073/FPJ-D-12-00062

Faruk, O., Bledzki, A. K., Fink, H. P., and Sain, M. (2012). "Biocomposites reinforced with natural fibers: 2000–2010," *Prog. Polym. Sci.* 37, 1552-1596. DOI: 10.1016/j.progpolymsci.2012.04.003

Hebel, D. E., Javadian, A., Heisel, F., Schlesier, K., Griebel, D., and Wielopolski, M. (2014). "Process-controlled optimization of the tensile strength of bamboo fiber composites for structural applications," *Compos. Part B: Eng.* 67, 125-131. DOI: 10.1016/j.compositesb.2014.06.032

Huda, S., Reddy, N., and Yang, Y. (2012). "Ultra-light-weight composites from bamboo strips and polypropylene web with exceptional flexural properties," *Compos. Part B: Eng.* 43, 1658-1664. DOI: 10.1016/j.compositesb.2012.01.017

Hung, K. C., Chen, Y. L., and Wu, J. H. (2012). "Natural weathering properties of acetylated bamboo plastic composites," *Polym. Degrad. Stabil.* 97, 1680-1685. DOI: 10.1016/j.polymdegradstab.2012.06.016

Lei, B., Zhang, Y., He, Y., Xie, Y., Xu, B., Lin, Z., Huang, L., Tan, S., Wang, M., and Cai, X. (2015). "Preparation and characterization of wood–plastic composite reinforced by

graphitic carbon nitride," *Mater. Design* 66 Part A, 103-109. DOI: 10.1016/j.matdes.2014.10.041

Li, X., Lei, B., Lin, Z., Huang, L., Tan, S., and Cai, X. (2014). "The utilization of bamboo charcoal enhances wood plastic composites with excellent mechanical and thermal properties," *Mater. Design* 53, 419-424. DOI: 10.1016/j.matdes.2013.07.028

Li, X., Lei, B., Lin, Z., Huang, L., Tan, S., and Cai, X. (2013). "The utilization of organic vermiculite to reinforce wood–plastic composites with higher flexural and tensile properties," *Ind. Crop. Prod.* 51, 310-316. DOI: 10.1016/j.indcrop.2013.09.019

Li, Y., Shen, H., Shan, W., and Han, T. (2012). "Flexural behavior of lightweight bamboo–steel composite slabs," *Thin Wall. Struct.* 53, 83-90. DOI: 10.1016/j.tws.2012.01.001

Liu, R., Peng, Y., Cao, J., and Chen, Y. (2014a). "Comparison on properties of lignocellulosic flour/polymer composites by using wood, cellulose, and lignin flours as fillers," *Compos. Sci. Technol.* 103, 1-7. DOI: 10.1016/j.compscitech.2014.08.005

Liu, R., Peng, Y., and Cao, J. (2014b). "A comparison of various ionic surfactant modifiers used in *in situ* synthesis of organo-montmorillonite inside wood flour," *Ind. Crop. Prod.* 62, 387-394. DOI: 10.1016/j.indcrop.2014.09.014

Lu, T., Liu, S., Jiang, M., Xu, X., Wang, Y., Wang, Z., Gou, J., Hui, D., and Zhou, Z. (2014). "Effects of modifications of bamboo cellulose fibers on the improved mechanical properties of cellulose reinforced poly(lactic acid) composites," *Compos. Part B: Eng.* 62, 191-197. DOI: 10.1016/j.compositesb.2014.02.030

Luo, H., Xiong, G., Ma, C., Chang, P., Yao, F., Zhu, Y., Zhang, C., and Wan, Y. (2014). "Mechanical and thermo-mechanical behaviors of sizing-treated corn fiber/ polylactide composites," *Polym. Test.* 39, 45-52. DOI: 10.1016/j.polymertesting.2014.07.014

Mamun, A. A., and Bledzki, A. K. (2013). "Micro fibre reinforced PLA and PP composites: Enzyme modification, mechanical and thermal properties," *Compos. Sci. Technol.* 78, 10-17. DOI: 10.1016/j.compscitech.2013.01.013

Ng, H. M., Sin, L. T., Tee, T. T., Bee, S. T., Hui, D., Low, C. Y., and Rahmat, A. R. (2015). "Extraction of cellulose nanocrystals from plant sources for application as reinforcing agent in polymers," *Compos. Part B: Eng.* 75, 176-200. DOI: 10.1016/j.compositesb.2015.01.008

Özşahin, Ş. (2012). "The use of an artificial neural network for modeling the moisture absorption and thickness swelling of oriented strand board," *BioResources* 7(1), 1053-1067. DOI: 10.15376/biores.7.1.1053-1067

Peng, Y., Liu, R., and Cao, J. (2015). "Characterization of surface chemistry and crystallization behavior of polypropylene composites reinforced with wood flour, cellulose, and lignin during accelerated weathering," *Appl. Surf. Sci.* 332, 253-259. DOI: 10.1016/j.apsusc.2015.01.147

Peng, Y., Liu, R., Cao, J., and Chen, Y. (2014). "Effects of UV weathering on surface properties of polypropylene composites reinforced with wood flour, lignin, and cellulose," *Appl. Surf. Sci.* 317, 385-392. DOI: 10.1016/j.apsusc.2014.08.140

Ren, W., Zhang, D., Wang, G., and Cheng, H. (2014). "Mechanical and thermal properties of bamboo pulp fiber reinforced polyethylene composites," *BioResources* 9(3), 4117-4127. DOI: 10.15376/biores.9.3.4117-4127

Saba, N., Paridah, M. T., and Jawaid, M. (2015). "Mechanical properties of kenaf fibre reinforced polymer composite: A review," *Constr. Build. Mater.* 76, 87-96. DOI: 10.1016/j.conbuildmat.2014.11.043

Verma, C. S., Sharma, N. K., Chariar, V. M., Maheshwari, S., and Hada, M. K. (2014). "Comparative study of mechanical properties of bamboo laminae and their laminates with woods and wood based composites," *Compos. Part B: Eng.* 60, 523-530. DOI: 10.1016/j.compositesb.2013.12.061

Wang, Y., Weng, Y., and Wang, L. (2014). "Characterization of interfacial compatibility of polylactic acid and bamboo flour (PLA/BF) in biocomposites," *Polym. Test.* 36, 119-125. DOI: 10.1016/j.polymertesting.2014.04.001

Wei, W., Song, W., and Zhang, S. (2014). "Preparation and characterization of hydroxyapatite-poly (vinyl alcohol) composites reinforced with cellulose nanocrystals," *BioResources* 9(4), 6087-6099. DOI: 10.15376/biores.9.4.6087-6099

Xie, Z., Chen, Y., Wang, C., Liu, Y., Chu, F., and Jin, L. (2014). "Effects of bio-based plasticizers on mechanical and thermal properties of PVC/wood flour composites," *BioResources* 9(4), 7389-7402. DOI: 10.15376/biores.9.4.7389-7402

Yeh, S. K., Hsieh, C. C., Chang, H. C., Yen, C. C. C., and Chang, Y. C. (2015). "Synergistic effect of coupling agents and fiber treatments on mechanical properties and moisture absorption of polypropylene–rice husk composites and their foam," *Compos. Part A: Appl. S.* 68, 313-322. DOI: 10.1016/j.compositesa.2014.10.019

Yildirim, I., Ozsahin, S., and Akyuz, K. C. (2011). "Prediction of the financial return of the paper sector with artificial neural networks," *BioResources* 6(4), 4076-4091. DOI: 10.15376/biores.6.4.4076-4091

Zainuddin, Z., Daud, W. R. W., Ong, P., and Shafie, A. (2012). "Pulp and paper from oil palm fronds: Wavelet neural networks modeling of soda-ethanol pulping," *BioResources* 7(4), 5781-5793. DOI: 10.15376/biores.7.4.5781-5793

Zakikhani, P., Zahari, R., Sultan, M. T. H., and Majid, D. L. (2014). "Extraction and preparation of bamboo fibre-reinforced composites," *Mater. Design* 63, 820-828. DOI: 10.1016/j.matdes.2014.06.058

Zhao, F. (2012). "Study on the key manufacture technology of bamboo plastic composites," M. S. Thesis, Beijing Forestry University, Beijing, China.

Zhou, X., Chen, L., and Lin, Q. (2012). "Effects of chemical foaming agents on the physico-mechanical properties and rheological behavior of bamboo powder-polypropylene foamed composites," *BioResources* 7(2), 2183-2198. DOI: 10.15376/biores.7.2.2183-2198

Article submitted: March 24, 2015; Peer review completed: June 10, 2015; Revised version received June 17, 2015; Accepted: June 20, 2015; Published: June 26, 2015.
DOI: 10.15376/biores.10.3.5049-5070